J Mater Sci (2008) 43:1688–1695
DOI 10.1007/s10853-007-2370-7

The energy required to ignite micropyretic synthesis. Part I: stable Ni + Al reaction

H. P. Li

Received: 8 February 2007 / Accepted: 3 December 2007 / Published online: 11 January 2008

Abstract The progression of chemical reactions is determined by both thermodynamics and kinetics factors. Micropyretic/combustion reaction is a cascade of many chain chemical reactions and thermodynamics and kinetics of the ignition reaction are expected to greatly affect the overall reaction outcome. Furthermore, the stability of the sequential reaction and its progression are correspondingly changed once micropyretic parameters are changed. Improper ignition of micropyretic reaction provides either excessive or insufficient external energy, thus causes over-heating or extinguishing of the combustion front during propagation and therefore the heterogeneous structures. To achieve the homogeneous micropyretic reaction, it is thought possible to control ignition energy. A numerical study on the correlation of thermodynamics and kinetics factors of ignition on the stable Ni + Al reaction and the required ignition energy is reported in this study. The influences of activation energy (E), enthalpy of the micropyretic reaction (Q), pre-exponential factor (K_o), thermal conductivity (K), heat capacity (C_p), and thermal activity of the reactants and product, on the temperature/heat loss at the ignition spot and the length of pre-heating zone are respectively studied. It is found that the activation energy and heat capacity have the most significant effects on the ignition energy. The required ignition energy is increased by 44.0% and 23.9%, respectively, when the activation energy and the heat capacity are both increased by 40.0%

H. P. Li (✉)
Jinwen University of Science and Technology, Hsintien, Taipei County 231, Taiwan, ROC
e-mail: hli@just.edu.tw

Introduction

Micropyretic/combustion synthesis is a novel processing technique in which the compacted powders are first ignited by an external heating source to induce the chemical reaction inside the heated materials [1–11]. After ignition, the energy to propagate the combustion front is obtained from the heat released by the formation of the synthesized product. The unreacted portion in front of the combustion front is heated by this exothermic heat, undergoes synthesis, and propagates, thus causing further reaction and synthesis. Improper ignition of the micropyretic reaction may offer excessive or insufficient external energy, causing over-heating or extinguishing of the front during propagation [11, 12]. Thus, appropriate ignition energy is required to propagate the stable combustion front. However, it has been also shown that the energy required to ignite the micropyretic reaction is strongly dependent on the ignition power and micropyretic reaction parameters [11]. To choose the appropriate ignition manner and further acquire the steady micropyretic reaction, an understanding of the correlation of each micropyretic synthesis parameter with the required ignition energy is important. This study aims at such an understanding.

The influences of the ignition manner on micropyretic synthesis have been investigated in several studies [13–18]. The experimental studies on the micropyretic reactions with 2Ni + Al [13] and Ti + Ni [14] systems have indicated that an increase in the ignition power increases the heating rate at the ignition spot. The temperature is quickly raised to the melting point of lower refractory reactant and then the melting of reactants accelerates to ignite the micropyretic reaction. Increasing the ignition power accelerates the rate of temperature increase up to the melting point of the reactants, thus reducing the ignition

time [13, 14]. Similar experimental results have been found in the Ti–C micropyretic reaction ignited by a mechanical milling [15]. It has also been shown that an increase in the milling energy decreases the ignition time. Another experimental investigation on Nb + C micropyretic reaction also shows that an increase in the ignition power reduces the ignition time; however, the energy for ignition is raised [16]. Shen et al. [13] reported that an increase in the reactant density increases the time for igniting the micropyretic reaction with 2Ni + Al. However, another study in the Ni + Al reaction showed different results [17]. It is shown that an increase in the compact pressure or the reactant density decreases the ignition temperature, further reducing the time required for ignition [17]. In addition to the compact density, the ratio of reactants [14] and the particle size [17, 18] both have been reported to influence the time required for ignition.

The previous numerical study has also shown that the energy required to ignite the Ti + 2B reaction is much higher than that required to ignite the Ni + Al reaction [11]. This is probably because the activation energy of Ti + 2B micropyretic reaction is higher than that of Ni + Al micropyretic reaction. However, it has been proposed that the activation energy, exothermic heat, pre-exponential factor, ignition power as well as thermophysical/chemical parameters of reactants and product probably influence the energy required to ignite the micropyretic reaction [11]. In order to understand the influence of the variations in these parameters on the ignition energy, the numerical investigation is systematically carried out to study the correlation of these parameters with the ignition energy during micropyretic synthesis. The correlations of these micropyretic parameters with thermal profiles are first investigated. In addition, the required energy to ignite the micropyretic reaction with these parameters is also calculated. The numerical procedure used in this study takes into consideration the various microprocesses, such as the melting of reactants, the diffusion and mixing of reactants, and the formation of products. The Ni + Al stable micropyretic reaction is chosen to demonstrate the effects on the ignition energy in this study.

Numerical calculation procedure

During the passage of a combustion front in the micropyretic reaction, the energy equation for transient heat conduction, which includes the source term containing heat release due to the exothermic reaction, is given as [1–3, 5]:

$$\rho C_p\left(\frac{\partial T}{\partial t}\right)=\frac{\partial}{\partial z}\left(\kappa\left(\frac{\partial T}{\partial z}\right)\right)-\frac{4h(T-T_o)}{d}+\rho Q\Phi(T,\eta) \quad (1)$$

Each symbol in the equation is explained in the nomenclature section. The reaction rate, $\Phi(T,\eta)$, in Eq. 1 is given as:

$$\Phi(T,\eta)=\frac{\partial\eta}{\partial t}=K_o(1-\eta)\exp\left(-\frac{E}{RT}\right) \quad (2)$$

In this study, a numerical calculation for Eq. 1 is carried out with the assumption of the first-order kinetics. In Eq. 1, the energy required for heating the synthesized product from the initial temperature to the adiabatic combustion temperature is shown on the left-hand side. The terms on the right-hand side are the conduction heat transfer term, the surface heat loss parameter, and the heat release due to the exothermic micropyretic reaction, respectively.

A middle-difference approximation and an enthalpy-temperature method coupled with Guass-Seidel iteration procedure are used to solve the equations of the micropyretic synthesis problems. In the computational simulation, a one-dimensional sample of 1 cm long is divided into 1,201 nodes (regions) to calculate the local temperature. This one-dimensional numerical model assumes the following sequence of events: (1) the specimen is gradually heated by a surface heat source in very small time steps (0.025 ms); (2) the reaction is ignited and the combustion front propagates along the specimen. The choice of 1 cm sample length is only for computational purpose and the simulation results are applicable to practical experimental conditions.

The various microscale events, that is, local processes such as heating of the sample, melting of lower refractory reactant, and formation of product, are included in this calculation procedure. In addition, the various thermophysical/chemical parameters, such as thermal conductivity, density, and heat capacity of the reactants and product, are assumed to be independent of temperature, but they are different in each state. The effect of melting of reactants and product is included in the calculation procedure. The porosities of the reactants and product which influence the density and thermal conductivity profiles are also considered in the calculation. The porosities of the reactants and product are both taken as 30% in this study. The average values of these parameters vary when the reaction proceeds, depending upon the degree of reaction. Depending on the values of the temperature and extent of enthalpy released in the reaction, the proper thermophysical/chemical parameters are considered in the numerical calculation. At any given time, the reacted fraction and the enthalpy of the current iteration are calculated from the previous reacted fraction, enthalpy, and other parameters of the earlier iteration. The range of the enthalpy as well as the molar ratio among each material for each node is thus determined, and the values of temperature, density, and thermal conductivity at each node can be further calculated

Table 1 The thermophysical/chemical parameters for the reactants and product at sold state (300 K) and liquid state [19–21]

Thermophysical/chemical parameters	Al	Ni	NiAl
Heat capacity (300 K) (J/(kgK))	902 [19]	445 [19]	537 [19]
Heat capacity (liquid) (J/(kgK))	1,178 [19]	735 [19]	831 [19]
Thermal conductivity (300 K) (J/(msK))	238 [21]	88.5 [21]	75 [20]
Thermal conductivity (liquid) (J/(msK))	100 [21]	53 [20]	55 [20]
Density (300 K) (kg/m^3)	2,700 [21]	8,900 [21]	6,050 [20]
Density (liquid) (kg/m^3)	2,385 [21]	7,905 [21]	5,950 [21]

in the appropriate zone. The criterion used to ascertain whether the reacted fraction (η) and the enthalpies (φ) at each time level converge or not, is determined from the relative error criterion, i.e., for all nodes $\left|(\eta^{t+1}-\eta^{t})/\eta^{t}\right| \le 10^{-6}$ and $\left|(\phi^{t+1}-\phi^{t})/\phi^{t}\right| \le 0.001$. The superscripts $t+1$ and t denote the current and previous iterations, respectively. Once the convergence criterion for every node is met, the enthalpy and the reacted fraction of the last iteration in a time step are considered to be the corresponding final values. The calculations are normally performed 500–2,000 times, depending upon the calculated thermal parameters to make all 1,201 nodes meet the criterion for each time step. At least 600 time steps are calculated to allow the propagation of the combustion front across the 1-cm-long specimen completely. The parameter values used in the computational calculation are shown in Tables 1 [19–21] and 2 [19, 22]. In this study, the combustion temperature is defined as the highest reaction temperature during combustion synthesis and the propagation velocity is the velocity of the combustion front propagation. The pre-heating zone is calculated from the end of reaction nodes (zones) until the position where the temperature is decreased to the original substrate temperature.

Results and discussion

Figure 1 shows the temperature profiles of combustion fronts at various times along the Ni + Al specimen. The micropyretic reactions are ignited by a constant heating rate of 397 Joule/(ms g) at the position 0 cm and the heating sources are removed immediately after the combustion front starts propagating from left to right. The interval time between two consecutive time steps (profiles) in Fig. 1 is 0.25 ms. Figure 1b shows that the combustion front takes 3.35 ms to start propagation for the reaction with the reported experimental activation energy (139.0 KJ/mole) [22]. This ignition time interval corresponds to the ignition energy of 1,330 Joule/g. When 80% of the reported experimental activation energy value (111.2 KJ/mole) is taken in the numerical calculation, the ignition time is reduced from 3.35 ms to 2.85 ms (Fig. 1a) and also the ignition energy is decreased to 983 Joule/g. In addition, the calculated propagation velocity is increased from 533 mm/s to 1,279 mm/s. On the other hand, the ignition time and energy are respectively increased to 3.80 ms and 1,578 Joule/g when 120% of the reported experimental activation energy is taken in the calculation (Fig. 1c). The combustion front is also noted to extinguish after ignition. Figure 1 indicates that the variations in activation energy change the ignition time and correspondingly affect the energy required to ignite the micropyretic reaction. Similarly, the changes in the other micropyretic parameters, including exothermic heat,

Table 2 The values of various parameters used in the numerical calculation [19, 22]

Parameters	NiAl
Combustion temperature (K)	1,912
Activation energy (kJ/mole)	139 [22]
Exothermic heat (kJ/mole)	118.5 [19]
Pre-exponential factor (1/s)	4×10^8

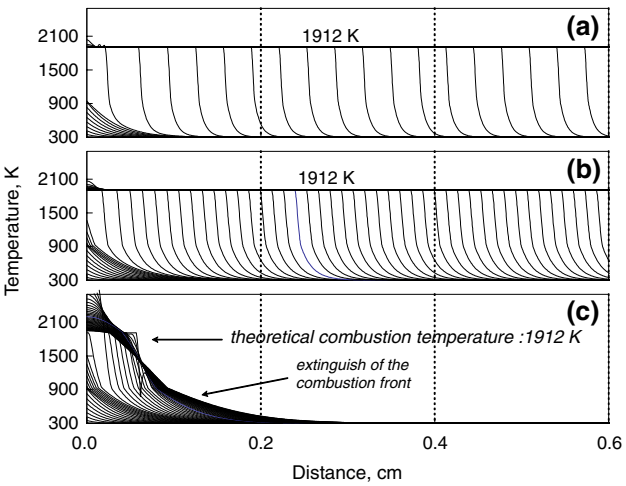

Fig. 1 Time variations of the combustion front temperature along the NiAl specimen with the pre-exponential factor of 4×10^8 s^{-1}. The interval time between two consecutive time steps (profiles) is 0.25 ms. The ignition power is taken as 397 Joule/(ms g) in the numerical calculation. The activation energy in (**a**), (**b**), and (**c**) are 111.2 KJ/mole (80% E), 139.0 KJ/mole (reported experimental value E) [22], and 166.8 KJ/mole (120% E), respectively

pre-exponential factor, heat capacity, thermal conductivity, and thermal activity, are expected to affect the ignition time and energy. To understand the impacts of the variations in these micropyretic parameters on the ignition condition, the influences of these parameters on the heat loss/temperature at the ignition point and the length of pre-heating zone are respectively studied in this article.

Activation energy

Figure 2a shows the temperature changes at the ignition point for the reactions with different values of activation energy. The initial heating rates at the ignition spot are calculated to be 260 K/ms. As temperature is increased to the melting point of Al ($T_{melting} = 933$ K), Al starts to melt and a temperature plateau is formed. The melting of Al increases the contact area between the reactants, further aiding the start of the micropyretic reaction and raising the temperature sharply. The micropyretic reaction with small activation energy (80% *E*, i.e., 80% of the reported experimental value) is found to ignite firstly and the temperature is then increased at 4,420 K/ms, as shown in Fig. 2a. An increase in the activation energy to 120% *E* decreases the kinetics of the reaction and further obstructs the start of the micropyretic reaction. The rate of temperature rise is thus decreased from 4,420 K/ms to 2,800 K/ms. Therefore, the time required for completing the reaction is increased, further correspondingly enhancing the required ignition energy for a given ignition power.

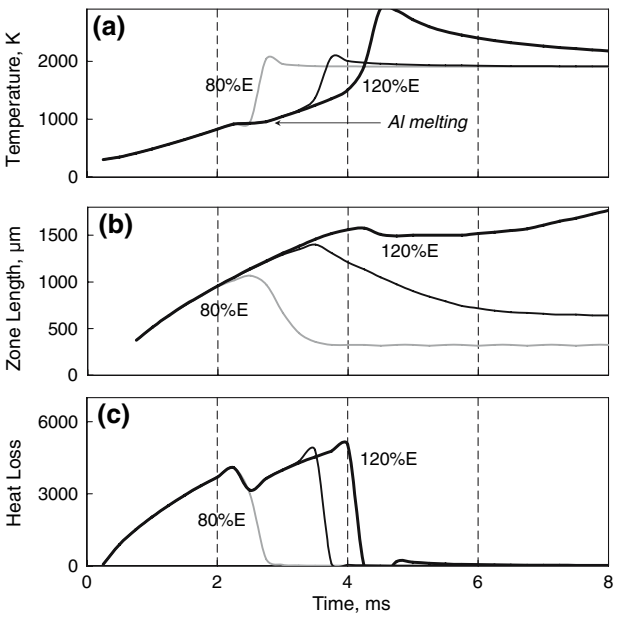

Fig. 2 The plots of (**a**) temperature at the ignition point, (**b**) length of pre-heating zone for a combustion front, and (**c**) dimensionless heat loss at the ignition point for the reactions with the different values of activation energy. The central line in each figure denotes the Ni + Al micropyretic reaction with the experimental value of activation energy 139 KJ/mole [22]. The other lines denote the reactions with 120% (bold line) and 80% of the reported value of activation energy, respectively

During heating of the sample, the thermal energy is continuously transferred from the reaction zone at ignition spot to the pre-heating zone. Thus, the temperature in the pre-heating zone is expected to enhance and zone length is correspondingly increased with the ignition time. Figure 2b shows that the length of pre-heating zone is continuously increased during the heating stage. After the micropyretic reaction is ignited, the heating source is immediately removed. The released exothermic heat replacing the heating source becomes the primary source to ignite the new reaction and provide the transferred energy to the pre-heating zone. Thus, the zone length is expected to remain constant with the propagation of a combustion front. Figure 2b shows that the zone length of a combustion front is gradually deceased to a constant value after the reaction is ignited. It is also noted that the reaction with smaller activation energy (80% *E*) is decreased first due to less ignition time. When a higher activation energy (120% *E*) is taken in the calculation, the ignition time and temperature are found to increase. Such an increase in the (initial) temperature at the ignition spot significantly raises the temperature higher than the theoretical combustion temperature (1,912 K) after the reaction is ignited, as shown in Fig. 2a. An abrupt increase in the temperature at the ignition spot is expected to lead to heterogeneous microstructure. The zone length is also found to continuously increase as the combustion front extinguishes.

Since the energy is continuously transferred (loss) from the ignition point to the pre-heating zone during heating of the specimen, the heat loss at the ignition point is therefore increased with the reaction time, as shown in Fig. 2c. It is noted that the heat loss distributions before the melting of Al for all the reactions are identical. When the temperature is increased to the melting point of Al, the temperature stops to increase and the heat loss is correspondingly decreased. As the reaction with lower activation energy (80% *E*) is ignited early at the melting point of Al, the reaction at the ignition spot is complete and heat loss is thus noted to decrease to zero during the Al melting. After the melting of reactant Al is complete, the heat loss is increased again for the reactions with higher activation energy. The increase in the heat loss is expected to enhance the energy required to ignite the micropyretic reaction.

Exothermic heat

Since the exothermic heat of the micropyretic reaction is released after the reaction has been ignited, it is not

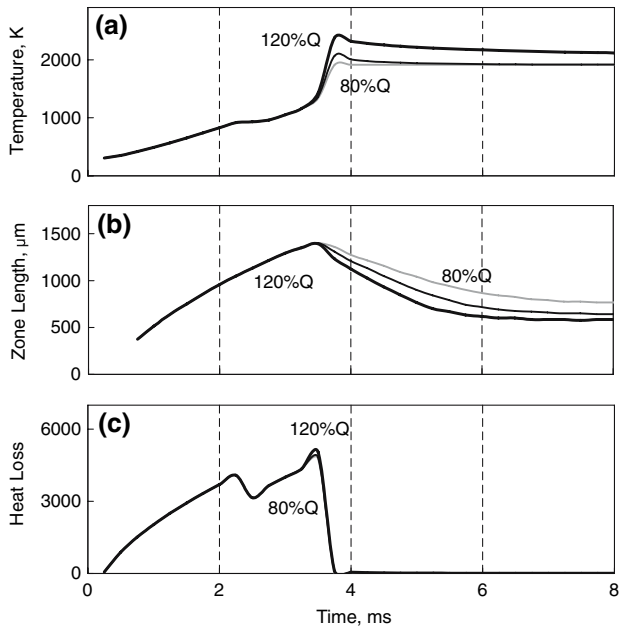

Fig. 3 The plots of (**a**) temperature at the ignition point, (**b**) length of pre-heating zone for a combustion front, and (**c**) dimensionless heat loss at the ignition point for the reactions with the different values of exothermic heat. The central line in each figure denotes the Ni + Al micropyretic reaction with the experimental value of exothermic heat 118.5 KJ/mole [19]. The other lines denote the reactions with 120% (bold line) and 80% of the reported value of exothermic heat, respectively

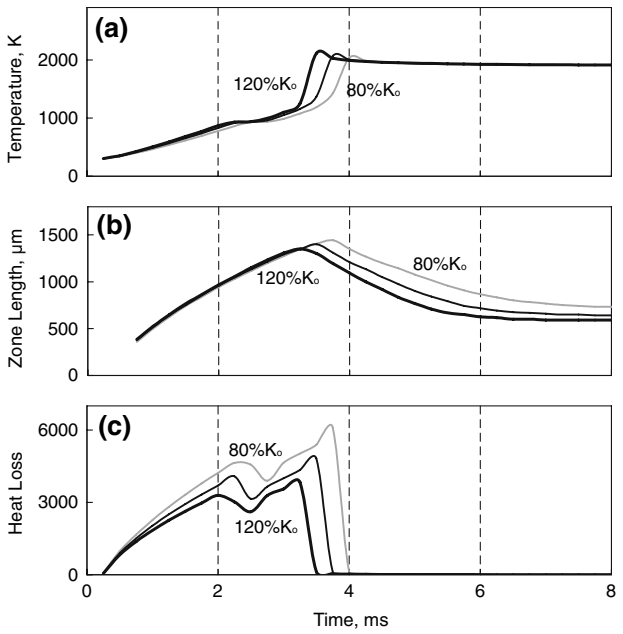

Fig. 4 The plots of (**a**) temperature at the ignition point, (**b**) length of pre-heating zone for a combustion front, and (**c**) dimensionless heat loss at the ignition point for the reactions with the different values of pre-exponential factor. The central line in each figure denotes the Ni + Al micropyretic reaction with the pre-exponential factor, 4×10^8 1/s. The other lines denote the reactions with 120% (bold line) and 80% of the value of pre-exponential factor, respectively

expected to influence the profiles of these studied parameters before the start of the micropyretic reaction. Hence, Fig. 3 shows that the temperature, zone length, and heat loss distributions are identical before the reactions are ignited. When the reaction is ignited and the exothermic heat is released, the temperature at the ignition spot is quickly enhanced. Figure 3a shows that the heating rate and combustion temperature (i.e., the highest temperature during the reaction) at the ignition spot are both increased with increasing exothermic heat. The higher exothermic heat of the micropyretic reaction leads to a higher combustion temperature and a faster propagation velocity. The faster propagation velocity corresponds to a narrower length of pre-heating zone. Hence, the stabilized constant value for zone length of combustion front is noted to decrease with the increase in the exothermic heat (Fig. 3b).

Pre-exponential factor

A change in the pre-exponential factor or frequency factor, K_o, is known to influence the reactivity of the micropyretic reaction [1, 2, 5]. The K_o value is reported to be proportional to D_o/r^2, where D_o is the reference diffusion coefficient and r is the diameter of the non-melting reactants [2]. An increase in the K_o value is equivalent to decreasing the particle size of the reactant or increasing the reference diffusion coefficient, which further increases the kinetics of the reaction. Hence, Fig. 4a shows that an increase in the pre-exponential factor reduces the time required to ignite the reaction and increases the propagating velocity. A narrower pre-heating zone is correspondingly formed, as shown in Fig. 4b. Since a smaller K_o value corresponds to a larger particle size of the reactant [5], the reaction with a smaller K_o value is expected to have a higher thermal conductivity for a given constituents and porosity. Thus, it is noted from Fig. 4c that the heat loss is increased with the decrease in the pre-exponential factor.

Thermal conductivity

The influences of the changes in the thermal conductivities of reactants and product are simultaneously considered in the calculation. Normally a lower thermal conductivity reduces the heat loss at the ignition spot and thus the reaction with a lower thermal conductivity is quickly ignited. Figure 5a illustrates that the ignition time is decreased as the thermal conductivity of reactants/product is decreased from the reported experimental value (100% K) to 80% of the reported value (80% K). The length of pre-heating zone (Fig. 5b) and the heat loss

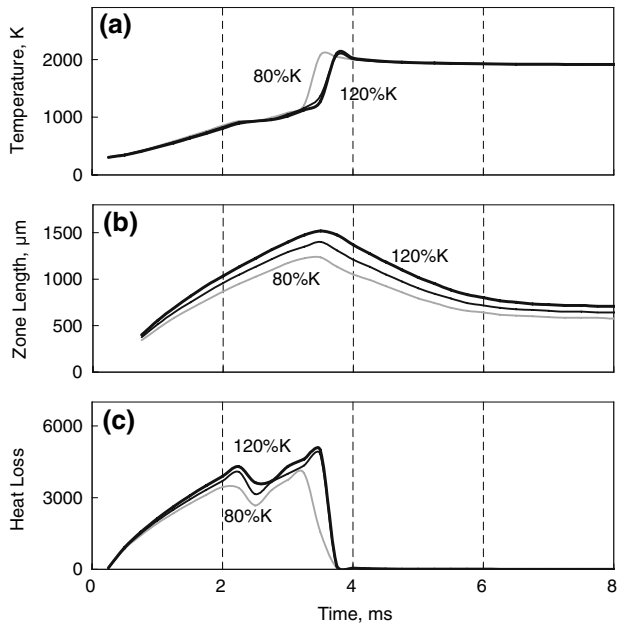

Fig. 5 The plots of (**a**) temperature at the ignition point, (**b**) length of pre-heating zone for a combustion front, and (**c**) dimensionless heat loss at the ignition point for the reactions with the different values of thermal conductivity. The central line in each figure denotes the Ni + Al micropyretic reaction with the experimental value of thermal conductivity. The other lines denote the reactions with 120% (bold line) and 80% of the experimental value of thermal conductivity, respectively

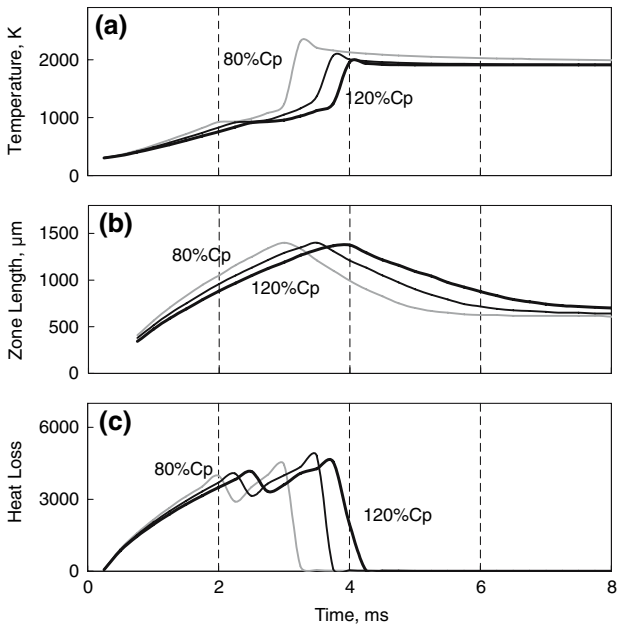

Fig. 6 The plots of (**a**) temperature at the ignition point, (**b**) length of pre-heating zone for a combustion front, and (**c**) dimensionless heat loss at the ignition point for the reactions with the different values of heat capacity. The central line in each figure denotes the Ni + Al micropyretic reaction with the experimental value of heat capacity. The other lines denote the reactions with 120% (bold line) and 80% of the experimental value of heat capacity, respectively

(Fig. 5c) are correspondingly reduced with the decrease in the thermal conductivity. The individual effect of thermal conductivity of reactants or product on the thermal profiles is also studied. The numerical results indicate that the changes in the temperature and heat loss at the ignition spot as well as the length of pre-heating zone are primarily influenced by the thermal conductivity of reactants. The variations in the thermal conductivity of product only slightly change the length of pre-heating zone after the reaction is ignited, whereas the amount of heat loss at the ignition spot is noted to be independent on the thermal conductivity of product.

Heat capacity

Figure 6 shows the distributions of temperature, zone length, and heat loss for the reaction with different heat capacities of reactants and product. The reaction with smaller heat capacity (80% C_p) is quickly heated for a given input energy. Thus, the rate of temperature increase is higher and the ignition time is correspondingly reduced with the decrease in heat capacity of reactants and product, as shown in Fig. 6a. Since the changes in the heat capacity do not affect the transfer of heat, the maximum values of the zone length (Fig. 6b) and heat loss (Fig. 6c) are almost the same for the reactions with different values of heat capacity. In other words, the heat capacity only affects the ignition time and the maximum values of heat loss and zone length are not influenced. Thus, the profiles for the reactions with different heat capacities of reactants and product are similar in the vertical direction and are only changed in the horizontal direction due to the different ignition time. The individual effect of heat capacities of reactants or product on these micropyretic parameters is also studied. As expected, the numerical results indicate that the heat capacity of reactants influences the studied micropyretic parameters before the start of micropyretic reaction whereas the heat capacity of product affects the micropyretic parameters after the start of reaction.

Thermal activity

In this study, the thermal activity is defined as the product of thermal conductivity, heat capacity, and porosity. Figure 7 indicates that with small thermal activity, the rate of temperature increase is slightly more at the ignition spot before ignition. It is also found that the profiles for the heat loss at the ignition spot and length of pre-heating zone are identical before the reaction starts. In addition, an increase in the thermal activity is also noted to increase the ignition time. The previous discussion has shown that the changes

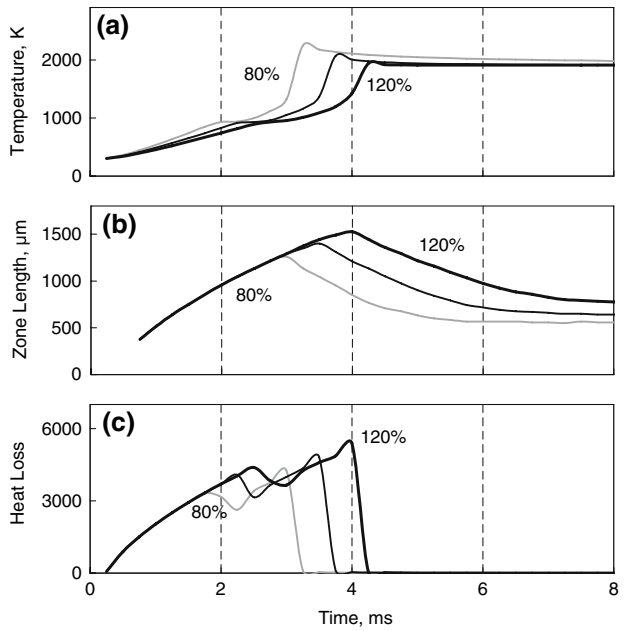

Fig. 7 The plots of (**a**) temperature at the ignition point, (**b**) length of pre-heating zone for a combustion front, and (**c**) dimensionless heat loss at the ignition point for the reactions with the different values of thermal activity. The central line in each figure denotes the Ni + Al micropyretic reaction with the experimental value of thermal activity. The other lines denote the reactions with 120% (bold line) and 80% of the experimental value of thermal activity, respectively

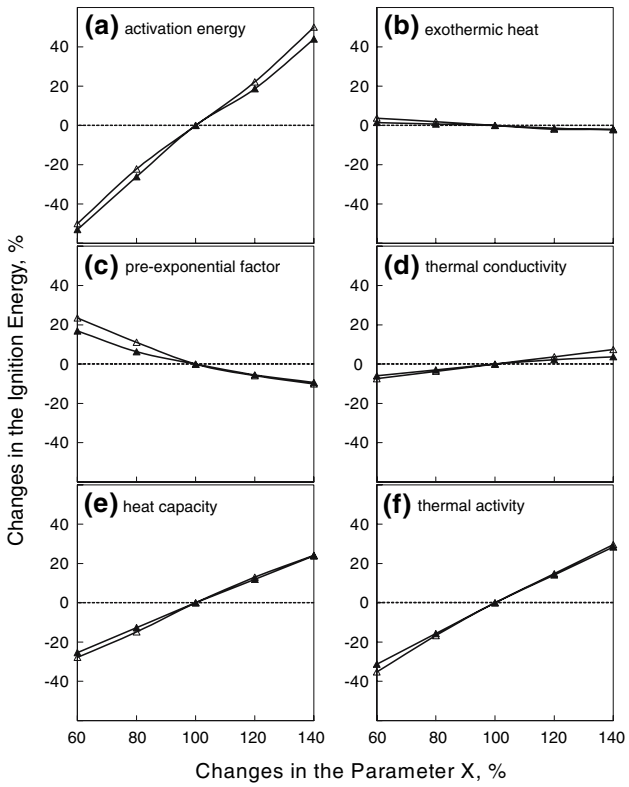

Fig. 8 The influence of the changes in the parameters (**a**) activation energy, (**b**) exothermic heat, (**c**) pre-exponential factor, (**d**) thermal conductivity, (**e**) heat capacity, and (**f**) thermal activity on the ignition energy. The NiAl micropyretic reactions are respectively ignited by a higher ignition rates of 1,911 Joule/(ms g) (solid symbols) and a lower ignition rates of 397 Joule/(ms g) (open symbols)

in thermal conductivity primarily affect the thermal profiles in the vertical direction (absolute value) whereas the changes in heat capacity affect the profiles in the horizontal direction (ignition time). Since the variations in the thermal activity is equivalent to the simultaneous changes in the thermal conductivity and the heat capacity, the changes in the profiles of temperature, heat loss, and zone length are found to vary both in the vertical and horizontal directions (Figs. 5–7).

Required ignition energy

The above numerical results have indicated that the micropyretic synthesis parameters have the pronounced effects on changing the temperature and further heat loss at the ignition spot. The time and energy required to ignite the micropyretic reaction are correspondingly altered by these micropyretic synthesis parameters. The influence of changing the parameters on the energy required to ignite the reactions are illustrated in Fig. 8. The calculated result indicates that 1,330 Joule/g and 1,608 Joule/g, respectively, are required to ignite the NiAl micropyretic reaction when the ignition rates of 397 Joule/(ms g) and 1,191 Joule/(ms g) are taken in the calculation. The required energy for the reaction ignited by a lower ignition rate is found to be less than that with a higher ignition rate. The calculated results agree with the experimental observation on the micropyretic reaction with Nb + C [16]. When the chosen parameters are increased to 140% and a lower ignition power (397 Joule/(ms g)) is taken in the calculation, Fig. 8 shows that the required ignition energy is increased by 44.0% for activation energy and 23.9% for heat capacity. Figure 8 illustrates that the ignition energy is slightly dependent on the exothermic heat/thermal conductivity and an increase in the pre-exponential factor decreases the required ignition energy. It is also noted that the percentage of change in the ignition energy for the reaction with different thermal activity is approximately equal to the sum of the change in ignition energy for the reactions with thermal conductivity and heat capacity.

Summary

A numerical investigation on ignition for synthesized NiAl compound has been studied in this article. The correlations of the heat loss/temperature at the ignition spot and the

length of pre-heating zone with the activation energy (E), exothermic heat (Q), pre-exponential factor (K_o), thermal conductivity (K), heat capacity (C_p), and thermal activity have been investigated. The variations in activation energy, E, has a pronounced effect on increasing the ignition time. It is found that the reaction with lower activation energy is ignited early at the melting of Al. A decrease in the ignition time further reduces the heat loss and ignition energy. The changes in the exothermic heat Q are noted to only affect the heat loss and zone length after the micropyretic reaction starts. Thus, the amount of the exothermic heat does not significantly affect the ignition energy. The pre-exponential factor K_o is reported to decrease the thermal conductivity. It is thus found that the rate of the heat loss is increased with decrease in the pre-exponential factor. The thermal conductivity and heat capacity are also noted to affect the heat loss at the ignition spot and length of pre-heating zone. An increase in the thermal conductivity increases the maximum value (vertical direction) of the heat loss and zone length whereas the heat capacity enlarges the distribution (shape) in the horizontal direction. When the changes in the thermal conductivity and the heat capacity are concurrently considered in the calculation, it is found that the variations in the thermal activity influence the thermal profiles and zone length in both directions. The required energy to ignite the micropyretic reactions with different micropyretic parameters is also calculated. An increase in the ignition power is noted to increase the required ignition energy. It is also found that the activation energy and heat capacity are the primary factors to influence the ignition energy. The calculated results also indicate that the percentage of change in the ignition energy for the reaction with different thermal activity is approximately equal to the sum of the change in ignition energy for the reaction with thermal conductivity and heat capacity.

Acknowledgements The supports from National Center for High-Performance Computing (account number: u48hpl00) and National Science Council (Grant number: NSC95-2221-E-228-002) in Taiwan are acknowledged.

References

1. Lakshmikantha MG, Bhattacharys A, Sekhar JA (1992) Metall Trans A 23A:23
2. Lakshmikantha MG, Sekhar JA (1993) Metall Trans A 24:617
3. Subramanian V, Lakshmikantha MG, Sekhar JA (1995) J Mater Res 10:1235
4. Munir ZA, Anselmi-Tamburini U (1989) Mater Sci Rep 3:277
5. Merzhanov AG, Khaikin BI (1988) Prog Energ Combust Sci 14:1
6. Li HP (2002) J Mater Res 17:3213
7. Li HP (2003) Acta Mater 51:3213
8. Li HP (2003) Metall Mater Trans A 34(9):1969
9. Li HP (2004) Scripta Mater 50(7):999
10. Li HP (2005) Chem Eng Sci 4:925
11. Li HP (2005) Acta Mater 53:2405
12. Lee WC, Chung SL (1995) J Mater Sci 30:1487
13. Shen P, Guo ZX, Hu JD, Lian JS, Sun BY (2000) Scripta Mater 43:893
14. Bertolino N, Monagheddu M, Tacca A, Giuliani P, Zanotti C, Tamburini UA (2003) Intermetallics 11:41
15. Deidda C, Delogu F, Maglia F, Anselmi-Tamburini U, Cocco G (2004) Mater Sci Eng A 375–377:800
16. He C, Stangle GC (1998) J Mater Res 13(1):135
17. Dong S, Hou P, Cheng H, Yang H, Zou G (2002) J Phys-Condens Mat 14(44):11023
18. Hunt EM, Plantier KB, Pantoya ML (2004) Acta Mater 52(11):3183
19. Brain I, Knacke O, Kubaschewski O (1973) Thermochemical properties of inorganic substances. Springer-Verlag, New York
20. Lide DR (1990) CRC handbook of chemistry, physics. CRC, Boca Raton
21. Brandes EA, Brook GB (1992) Smithells metals reference book. Butterworth-Heinemann Ltd
22. Naiborodenko YS, Itin VI (1975) Combust Explos Shock Waves 11(3):293